Mechanics of Advanced Composite Structures 9 (2022) 173 – 184

Semnan University

Mechanics of Advanced Composite Structures

journal homepage: http://MACS.journals.semnan.ac.ir

Investigation of Free Vibration of Laminated Composite Conical Shell with Local Attached Mass

R. Azarafza *, A. Davar, H. Baghani

Faculty of Materials & Manufacturing Technologies, Malek Ashtar University of Technology, Tehran, Iran.

KEYWORDS

Attached mass;
Composite conical shell;
Free vibration;
Galerkin method.

ABSTRACT

In this paper, for the first time, the free vibrations of the conical shell with the locally attached mass are investigated. The equilibrium equations of the conical shell are written based on classical shell theory using the energy method and Hamilton's principle. Boundary conditions are considered to be fully simply supported. According to the boundary conditions, the displacement components are written as double Fourier series expansions. Relationships of the strain-displacement and curvature-displacement are considered based on first Love's approximation theory. The governing equations of the conical shell are solved using the Galerkin method and the natural frequencies are obtained. Also, for the first time, the effect of the attached mass using the cone differential operator and Heaviside function on equilibrium equations has been considered and its effect on the free vibration of the conical shell has been investigated. The results have been verified with the literature and ABAQUS finite element software. Finally, the effect of different parameters of attached mass including width, height, subtended angle, position, density, and elastic modulus on the free vibrations of the composite conical shell are investigated.

1. Introduction

Shells are one of the most structures widely used in the space industry. In order to benefit from proper aerodynamic properties, a conical shell is used in these industries. For example, the conical shell used in satellite carriers in the space industry is one of the applications of this type of shell. Sometimes, to improve the performance of the shell, part of it is reinforced. The reinforcement has hardness and mass, which are effective parameters on the natural frequency. Therefore, in order to prevent the phenomenon of resonance and disturbance in the performance of the components attached to the shell, it is important to know the natural frequencies of the conical shell with the attached mass. Extensive research has been done on the free vibrations of conical shells and the effect of the mass attached to the plates and shells.

Tong [1] has investigated free vibration of composite laminated conical shells, with orthotropic stretching-bending coupling by using a particular coordinate system and a simple and exact solution obtained directly. Shu [2] has calculated the endeavor to apply the global method of generalized differential quadrature to the free vibration analysis of composite laminated conical shells. Love's first approximation thin shell theory is used to formulate the governing equations. The fundamental frequency parameters for four sets of boundary conditions and various shell thicknesses and different numbers of layers are presented.

Li et al. [3] have investigated free and forced vibration responses of a conical shell. Hamilton's principle with the Rayleigh-Ritz method is used to derive the equation of motion of the conical shell. Jin et al. [4] have modified the Fourier series using auxiliary functions to solve the free vibrations of the conical shell in order to solve the problem of Fourier series discontinuity in individual derivatives and using the Rayleigh-Ritz method, they showed that conical shells with arbitrary boundary conditions including all

* Corresponding author. Tel.: +98-9126479404: Fax: 98-21-22932256.
E-mail address: azarmut@mut.ac.ir , azarkntu@yahoo.com.

DOI: 10.22075/macs.2022.23203.1336
Received 2021-04-20; Received in revised form 2022-01-21; Accepted 2022-02-21.

classical and elastic end restraints can be solved in a unified form. Nasiri Rad et al. [5] by using the Galerkin method and considering the shape functions of the beam modes as weight functions analyzed the free and forced vibrations of the composite conical shell. Nallim et al [6] have investigated the effect of attached mass in the center of the isotropic and orthotropic circular plate on vibrations, regardless of their stiffness. Bambill et al. [7] investigated the effect of attached mass at an arbitrary position on the transverse vibrations of circular and annular plates by analytical and experimental methods. They also did not include the effect of mass stiffness in the equations and their studies, they have investigated the effect of mass distance from the center of the circle to the abutment. Amabili et al. [8] investigated the effect of concentrated masses with rotary inertia on vibrations of rectangular plates by experimental and numerical methods. Boundary conditions are considered simply supported and fixed. Ciancio et al. [9] studied the free vibration analysis of a cantilevered rectangular anisotropic plate when a concentrated mass is rigidly attached to its center point. Based on the classical theory of anisotropic plates, the Ritz method is employed to perform the analysis. Khalili et al. [10] are analyzed free vibrations of a cross-ply composite shell with or without a uniformly distributed attached mass using higher-order shell theory. The stiffness effect of this distributed attached mass is also considered. They showed that the effect of the stiffness of the distributed attached mass is decreased by decreasing the radii of curvatures or increasing the thickness of the shells. Aksencer and Aydogdu [11] have investigated the vibration of a rotating composite beam with an attached point mass. The Ritz method with algebraic polynomials is used in the formulation. The boundary conditions are considered clamped-free. Qu et al. [12] investigated the free vibration characteristics of conical-cylindrical-spherical shells combinations with ring stiffeners by using a modified variational method. Reissner- Naghdis thin shell theory in conjunction with a multilevel partition technique is employed to formulate the theoretical model. Nekouei et al. [13] studied the free vibration analysis of laminated composite conical shells reinforced with shape memory alloy fibers. Love's first approximation classical shell theory with the von-Kármán type of geometrical nonlinearity is used in conjunction with Hamilton's principle for deriving the equations of motion. Song et al. [14] studied free vibration of truncated conical shells with arbitrary boundary conditions, including elastic and inertia force constraints. The equations of motion with elastic boundary constraints are formulated by employing Hamilton's principle and the thin-walled shallow shell theory of the Donnell type.

In this paper, the free vibrations of a composite conical shell with a locally attached mass are investigated by using classical shell theory and finite element software ABAQUS and the results are compared. The effect of the attached mass on the free vibrations of the conical shell is defined using the property of the Heaviside function. To satisfy the boundary conditions, the displacement components are considered as double Fourier series. In addition, the effect of the attached mass and geometric parameters on the natural frequencies of the conical shell are also investigated. The proposed method applies to attached circular and sectorial circumferential ribs and longitudinal stringers with full or partial cone length. The main novelty of the present work is the application of the Heaviside step function idea for mathematical modeling of the mass and stiffness of circumferential ribs and longitudinal stringers.

2. Governing Equation

Figure 1 shows a conical shell with a small radius R_1, large radius R_2, thickness h, and semi-vertex angle φ.

Figure 2 also shows the conical shell with the attached mass. The center point of the attached mass on the shell in the form of an arc of subtended angle (θ) is located at distance (x) from the vertex.

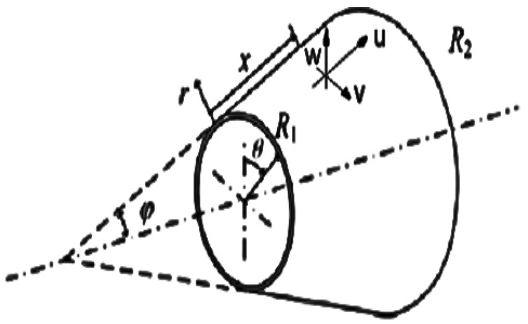

Fig. 1. Coordinates of the conical shell [4]

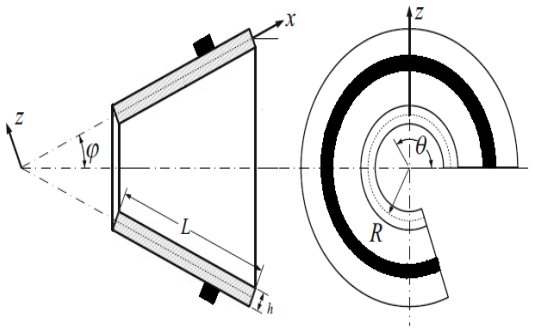

Fig. 2. Shell with the attached mass [10]

The large radius of the shell changes according to the length of the edge of the conical shell, which is obtained using Equation (1):

$$R(x) = R_1 + x \cdot \sin(\varphi) \tag{1}$$

The u ,v and w are the displacement components in the axial, tangential, and radial direction respectively, and the deformations are assumed to be small. Based on the classical shell theory equilibrium equations are as follows [2, 4]:

$$\begin{aligned}
&\frac{\partial N_x}{\partial x} + \frac{\sin\phi}{R(x)}(N_x - N_\theta) + \frac{1}{R(x)}\frac{\partial N_{x\theta}}{\partial \theta} = I_1 \frac{\partial^2 u}{\partial t^2} \\
&\frac{\partial N_{x\theta}}{\partial x} + \frac{1}{R(x)}\frac{\partial N_\theta}{\partial \theta} + \frac{2\cdot\sin(\phi)}{R(x)} N_{x\theta} + \frac{\cos(\phi)}{R(x)} Q_\theta = I_1 \frac{\partial^2 v}{\partial t^2} \\
&-\frac{\cos(\phi)}{R(x)} N_\theta + \frac{\partial Q_x}{\partial x} + \frac{\sin(\phi)}{R(x)} Q_x + \frac{1}{R(x)}\frac{\partial Q_\theta}{\partial \theta} = I_1 \frac{\partial^2 w}{\partial t^2}
\end{aligned} \tag{2}$$

where Q_x and Q_θ are defined by the following relations:

$$\begin{aligned}
Q_x &= \frac{\partial M_x}{\partial x} + \frac{\sin(\phi)}{R(x)}(M_x - M_\theta) + \frac{1}{R(x)}\frac{\partial M_{x\theta}}{\partial \theta} \\
Q_\theta &= \frac{1}{R(x)}\frac{\partial M_\theta}{\partial \theta} + \frac{2\sin(\phi)}{R(x)} M_{x\theta} + \frac{\partial M_{x\theta}}{\partial x}
\end{aligned} \tag{3}$$

In the above equation, I_1 is defined as follows:

$$I_1 = \int_{-\frac{h}{2}}^{\frac{h}{2}} \rho_k dz \tag{4}$$

where h is the laminate thickness and ρ_k is the density of each layer (The subscript "k" is the layer number). Constitutive equations of the composite shell are defined by the following relations [15]:

$$\begin{aligned}
\begin{Bmatrix} N_x \\ N_\theta \\ N_{x\theta} \end{Bmatrix} &= \begin{bmatrix} A_{11} & A_{12} & A_{16} \\ A_{12} & A_{22} & A_{26} \\ A_{16} & A_{26} & A_{66} \end{bmatrix} \begin{Bmatrix} \varepsilon_x^0 \\ \varepsilon_\theta^0 \\ \gamma_{x\theta}^0 \end{Bmatrix} + \begin{bmatrix} B_{11} & B_{12} & B_{16} \\ B_{12} & B_{22} & B_{26} \\ B_{16} & B_{26} & B_{66} \end{bmatrix} \begin{Bmatrix} K_x^0 \\ K_\theta^0 \\ K_{x\theta}^0 \end{Bmatrix} \\
\begin{Bmatrix} M_x \\ M_\theta \\ M_{x\theta} \end{Bmatrix} &= \begin{bmatrix} B_{11} & B_{12} & B_{16} \\ B_{12} & B_{22} & B_{26} \\ B_{16} & B_{26} & B_{66} \end{bmatrix} \begin{Bmatrix} \varepsilon_x^0 \\ \varepsilon_\theta^0 \\ \gamma_{x\theta}^0 \end{Bmatrix} + \begin{bmatrix} D_{11} & D_{12} & D_{16} \\ D_{12} & D_{22} & D_{26} \\ D_{16} & D_{26} & D_{66} \end{bmatrix} \begin{Bmatrix} K_x^0 \\ K_\theta^0 \\ K_{x\theta}^0 \end{Bmatrix}
\end{aligned} \tag{5}$$

where A, B, and D are extensional, coupling, and bending stiffness matrices, respectively, defined as follows [15]:

$$\left(A_{ij}, B_{ij}, D_{ij}\right) = \int_{-\frac{h}{2}}^{\frac{h}{2}} \left(1, z, z^2\right) \overline{Q}_{ij} dz \qquad (i, j = 1, 2, 6) \tag{6}$$

where $\overline{Q}_{ij}$ is the transformed reduced stiffness matrix (and are shown in Appendix A), ε_x^0 , ε_θ^0 , and $\varepsilon_{x\theta}^0$ are the mid-surface engineering strains and K_x^0 , K_θ^0 , and $K_{x\theta}^0$ are curvatures of mid-surface of the shell. Considering $x = R(x)/\sin(\varphi)$, the strains and curvatures are defined by the following relations [16]:

$$\begin{aligned}
&\varepsilon_x^0 = \frac{\partial u}{\partial x} \\
&\varepsilon_\theta^0 = \frac{1}{R(x)}\frac{\partial v}{\partial \theta} + \frac{\sin(\phi)}{R(x)} \cdot u + \frac{\cos(\phi)}{R(x)} \cdot w \\
&\varepsilon_{x\theta}^0 = \frac{\partial v}{\partial x} + \frac{1}{R(x)}\frac{\partial u}{\partial \theta} - \frac{\sin(\phi)}{R(x)} v \\
&K_x^0 = -\frac{\partial^2 w}{\partial x^2} \\
&K_\theta^0 = \frac{\cos(\phi)}{R(x)^2}\frac{\partial v}{\partial \theta} - \frac{1}{R(x)^2}\frac{\partial^2 w}{\partial \theta^2} - \frac{\sin(\phi)}{R(x)}\frac{\partial w}{\partial x} \\
&K_{x\theta}^0 = \frac{\cos(\phi)}{R(x)}\frac{\partial v}{\partial x} - \frac{2\cos(\phi)\cdot\sin(\phi)}{R(x)^2} v \\
&\quad -\frac{2}{R(x)}\frac{\partial^2 w}{\partial x \partial \theta} + \frac{2\sin(\phi)}{R(x)^2}\frac{\partial w}{\partial \theta}
\end{aligned} \tag{7}$$

3. Boundary Condition

The boundary conditions for the conical shell with fully simply supported (SS) at $x = 0$ and $x = L$ are considered as:

$$\begin{aligned}
v &= 0 \qquad w = 0 \\
N_x &= 0 \qquad M_x = 0
\end{aligned} \tag{8}$$

In order to satisfy the boundary conditions, u , v and w are defined by the following double Fourier series :

$$\begin{aligned}
u &= \sum_m \sum_n U \cdot f_{11}(x,\theta) \cdot f(t) \\
v &= \sum_m \sum_n V \cdot f_{21}(x,\theta) \cdot f(t) \\
w &= \sum_m \sum_n W \cdot f_{31}(x,\theta) \cdot f(t)
\end{aligned} \tag{9}$$

In the above equations, $f(t)$ is a periodic function of time and based on the type of the boundary conditions, f_{11}‘ f_{21} and f_{31} are determined as follows [17]:

$$\begin{aligned}
f_{11} &= \varphi_u(x)\phi_u(\theta) \\
f_{21} &= \varphi_v(x)\phi_v(\theta) \\
f_{31} &= \varphi_w(x)\phi_w(\theta)
\end{aligned} \tag{10}$$

where ϕ_u ‘ϕ_v‘ϕ_w and φ_i are trigonometric functions in the circumferential direction and defined by the following relations [15]:

$$\begin{aligned}
&\phi_u(\theta) = \phi_v(\theta) = \cos(n\theta) \\
&\phi_v(\theta) = \sin(n\theta) \\
&\varphi_i(x) = \alpha_1 \cosh\left(\frac{\lambda_m x}{L}\right) + \alpha_2 \cos\left(\frac{\lambda_m x}{L}\right) - \\
&\quad \sigma_m\left(\alpha_3 \sinh\left(\frac{\lambda_m x}{L}\right) - \alpha_4 \sin\left(\frac{\lambda_m x}{L}\right)\right), i = u, v, w
\end{aligned} \tag{11}$$

where α_i, λ_m and σ_m could be obtained from the boundary conditions. Finally, for SS boundary conditions, displacement components are defined as follows [17]:

$$\begin{aligned} u &= U_{mn} \cdot \cos\left(\frac{m\pi x}{L}\right) \cdot \cos(n\theta) \cdot f(t) \\ v &= V_{mn} . \sin\left(\frac{m\pi x}{L}\right) \cdot \sin(n\theta) \cdot f(t) \\ w &= W_{mn} . \sin\left(\frac{m\pi x}{L}\right) \cdot \cos(n\theta) \cdot f(t) \end{aligned} \quad (12)$$

where U_{mn}, V_{mn} and W_{mn} are the constant coefficients of the natural mode shapes associated with the free vibration problems, m is the axial half-wave, and m is the circumferential wave number. By using Eqs. (4) and (6) and substituting them in the equilibrium equations, the following equation is obtained:

$$[L]\{U\} = [I]\frac{\partial^2}{\partial t^2}\{U\}$$

$$L = \begin{bmatrix} L_{11} & L_{12} & L_{13} \\ L_{21} & L_{22} & L_{23} \\ L_{31} & L_{32} & L_{33} \end{bmatrix} \qquad \{U\} = \begin{Bmatrix} u(x,\theta,t) \\ v(x,\theta,t) \\ w(x,\theta,t) \end{Bmatrix} \quad (13)$$

$$I = \begin{bmatrix} I_1 & 0 & 0 \\ 0 & I_1 & 0 \\ 0 & 0 & I_1 \end{bmatrix}$$

Those L_{ij} are the differential operators and are shown in Appendix B. For solving Eq. (13), the Galerkin method is used.

4. Free Vibration Analysis

To solve the free vibration analysis, the function of time is treated as $f(t) = e^{i\omega_{mn}t}$ where ω_{mn} is the natural frequency. By substituting Eq. (12) into Eq. (13) and using the Galerkin method and after simplification, the following equation is obtained:

$$\left[\left[K_{ij}\right] - \omega^2{}_{mn}\left[M_{ij}\right]\right]\{U_{mn} \quad V_{mn} \quad W_{mn}\}^T = 0 \quad (14)$$

Those $[K_{ij}]$ and $[M_{ij}]$ are stiffness and mass matrices. By setting determinant of coefficients equal to zero, the characteristic frequency equation is derived as:

$$\beta_1 \omega_{mn}{}^6 + \beta_2 \omega_{mn}{}^4 + \beta_3 \omega_{mn}{}^2 + \beta_4 = 0 \quad (15)$$

where β_i are constant coefficients. By solving Eq. (15), natural frequencies are calculated, and by substituting these frequencies in Eq. (14), the constant coefficients of mode shapes are obtained.

5. Attached Mass Analysis

The assumption of concentrated mass directly affects the stiffness and mass matrices of the system. Therefore, it should be added to the equilibrium equations of the shell in such a way that the effect of the mass is distributed at the place of its application and not in the whole shell. For this purpose, the Heaviside function is used [10] as follows:

$$H(x - x_0,\ \theta - \theta_0) = \begin{Bmatrix} 1 \text{ at } x \geq x_0 & , \theta \geq \theta_0 \\ 0 \text{ at } x < x_0 & , \theta < \theta_0 \end{Bmatrix} \quad (16)$$

So the equations of motion change as follows:

$$[Lij]_s\{U\} + H(x,\theta,x_0,\theta_0,c,d)[Lij]_a\{U\} = [I_1]\frac{\partial^2}{\partial t^2}\{U\} + H(x,\theta,x_0,\theta_0,c,d)[I_1]\frac{\partial^2}{\partial t^2}\{U\} \quad (17)$$

Eq. (17), the index s stands for the shell and the index a stands for the attached mass. α_0 and θ_0 are coordinates of the position of the center of the mass, c and d are dimensions of the mass. Accordingly, H is Heaviside function and defined as follows:

$$H(x,\theta,x_0,\theta_0,c,d) = \left[H(x - x_0) - H(x - x_0 - c)\right] \times \left[H(\theta - \theta_0) - H(\theta - \theta_0 - d)\right] \quad (18)$$

In order to solve Eq. (17), the Galerkin method is used and the effect of the Heaviside function on the integrals of this method is as follows:

$$\int_0^a \int_0^b H \cdot f(x,\theta)\, dx d\theta = \int_{\theta_0}^{\theta_0 + d} \int_{x_0}^{x_0 + c} f(x,\theta)\, dx d\theta \quad (19)$$

In the above relation, a and b are the size of the attached mass (in angular and longitudinal directions, respectively).

6. Modeling and Analysis in ABAQUS Software

To check the accuracy of the results obtained from the free vibrations analysis as well as the shell with the attached mass, the composite conical shell is modeled in ABAQUS software as shown in Figure 3. In finite element software, S4R type element is used to mesh the shell and the attached mass.

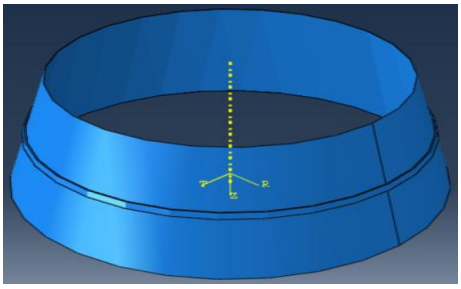

Fig. 3. Conical shell model with attached mass in ABAQUS software

The boundary condition at the two ends of the shell is simply supported. Since in this study, the free vibration analysis of the structure is considered by defining a frequency step, no force is defined and only the constraints of the support are applied. In finite element software, the shell element is used and for this element, six degrees of freedom are defined in each node, of which three degrees of freedom are transitional and three degrees of freedom are related to rotational motion. According to the defined coordinate system, only constraints are enough to achieve a simple boundary condition, U3 and UR2 in ABAQUS are free and the others are fixed. Here a tie constraint is applied between the surfaces of the shell and attached mass that are in contact with each other.

7. Results and Discussions of Numerical Analysis

To verify the accuracy of the results of this study, the validity of the results has been done in two ways. First, for free vibrations of the conical shell (ignoring the attached mass), a comparison with the results of the previous researches and numerical simulations in ABAQUS software have been performed. The present analytical results for isotropic conical shell vibrations with attached mass obtained from the analytical method are validated with the numerical simulation results in ABAQUS software. The mechanical properties and geometric characteristics of the conical shell in this study are given in Tables 1 and 2, respectively. Specifications of the attached mass are listed in each case.

Table 1. The mechanical properties of the shell

Material Number	E_{11} (GPa)	E_{22} (GPa)	$G_{12}=G_{13}$ (GPa)	G_{23} (GPa)	ν_{12}	$\rho(\frac{kg}{m^3})$
1	181	10.3	7.12	2.5	0.28	7
2	70	70	26.92	26.92	0.3	2710

Table 2. Geometric characteristics of the shell (mm)

Geometry	R_1	L	h	Layup
1	1	1	0.002	[90/0/90/0/90/0]
2	0.3	-	0.004	isotropic

7-1- Free Vibration of Conical Shell

For comparison with references and validation, the natural frequencies are presented in dimensionless form $(F=\omega_0 R_2\sqrt{\rho\left(1-\upsilon^2\right)/E})$. In this relation, ω_0 is the natural frequency (rad/s), R_2 is the large radius of the conical shell, h is the thickness, L is the edge length, m and n are the axial half-wave and the circumferential wave numbers, respectively. The results obtained for the isotropic conical shell using the present analytical method (using a MATLAB code) have been compared with other references in Tables 3 to 5 with different semi-vertex angles.

Table 3. Compression of dimensionless frequency material no.2, geometry no.2, $\varphi=30^{\circ}$, $L=0.2\,m$, $m=1$

n	Ref. [3]	Present	%Error
2	0.8420	0.8405	0.17
3	0.7376	0.7375	0.01
4	0.6362	0.6368	0.09
5	0.5528	0.5536	0.14
6	0.4950	0.4955	0.1
7	0.4661	0.4661	0
8	0.4660	0.4653	0.15

Table 4. Compression of dimensionless frequency material 2, geometry no. 2, $\varphi=45^{\circ}$, $L=0.14\,m$, $m=1$

n	Ref. [3]	Present	%Error
2	0.7655	0.7639	0.2
3	0.7212	0.7205	0.09
4	0.6739	0.6738	0.01
5	0.6323	0.6326	0.04
6	0.6035	0.6038	0.01
7	0.5921	0.5920	0.01
8	0.6001	0.5995	0.09

Table 5. Compression of dimensionless frequency material no. 2, geometry no.2, $\varphi=60^{\circ}$, $L=0.11\,m$, $m=1$

n	Ref. [3]	Present	%Error
2	0.6348	0.6341	0.06
3	0.6238	0.6243	0.06
4	0.6145	0.6143	0.03
5	0.6111	0.6109	0.03
6	0.6171	0.6168	0.04
7	0.6350	0.6344	0.09
8	0.6660	0.6649	0.16

Also, in Figure 4, the natural frequencies of the conical composite shell obtained from the present method are compared with ABAQUS software. As can be seen from the figure, the results are in good agreement.

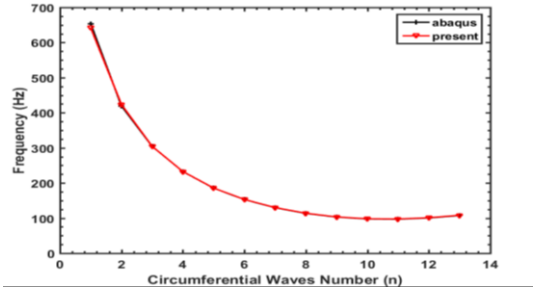

Fig. 4. Comparison of the frequency of composite conical shell for material no. 1, geometry no.1, $m=1$

7-2- Free Vibration of Conical Shell with Attached Mass

To ensure the accuracy of the present method for a shell with attached mass, in a special case the conical shell with a zero semi-vertex angle ($\varphi = 0^{\circ}$ or cylindrical shell), natural frequencies of the shell with the attached mass that obtained with the present method was compared with Ref. [18]. The geometrical dimensions and material properties of the shell model are given in Table 6. This model is an externally ring stiffened cylindrical shell. Table 7 shows the comparison of present analytical results of natural frequencies with Ref. [18]. The good agreement between the present results and Ref. [18].

Table 6. Geometrical and material properties of the stiffened shell

Characteristics	Physical dimensions and values
Number of rings	19
Shell radius (m)	0.049759
Shell thickness (m)	0.001651
Shell length (m)	0.3945
Rings height (m)	0.005334
Rings width (m)	0.003175
Modulus of elasticity (GPa)	68.95
Mass density (kg/m3)	2762
Poisson's ratio	0.3

Table 7. Comparison of natural frequencies obtained with the present method with Ref. [18](for the shell with attached mass)

n	Frequency [Hz]		%Error
	Present	Ref. [18]	
1	1217.6	1199.58	%1.5
2	1555.6	1564.47	%0.5
3	4284.6	4387.59	%2.34
4	8083.1	8377.75	%3.5
5	13005.4	13490.7	%3.6

In this part, the free vibration of the shell considering the effect of the attached mass is examined without considering its stiffness. Figure 5 shows the results of the vibration analysis of an isotropic cone of material no. 2 in which an attached mass with geometric properties $\rho_a = 10\,\rho_s$, $\theta_a = 2\pi$, $L_a = 0.05\,m$ and $h_a = 0.002$ is located in the center of the cone. The subscript (a) stands for the attached mass and subscript (s) stands for the shell. According to the figure, the addition of the mass attached to the conical shell has reduced the frequencies in all circumferential modes. In the case of the shell with attached mass, the results are compared with ABAQUS. The greatest discrepancy is related to the zero circumferential mode (n=0) and it is 16.3% as indicated in Figure 5.

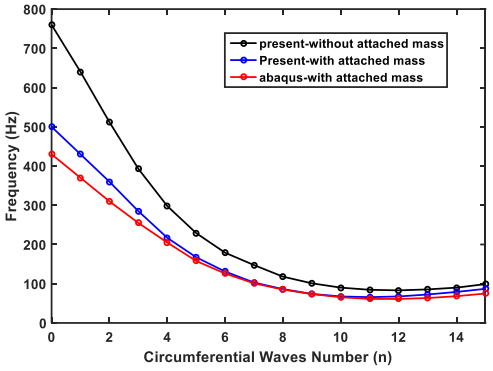

Fig. 5. Comparison of analytical and numerical results of isotropic conical shell frequency with attached mass for different circumferential modes, material no. 2, geometry no. 2, m=1, $\varphi_s = 30^{\circ}$

At this stage of the analysis, a conical composite shell is considered and the attached mass is placed on the conical shell and the effect of various parameters such as width, height, mass angular position around the cone, full ring, stringer and mass distance from the support to the composite conical shell have been investigated.

First, the attached mass is placed at the middle of the conical shell as a segment of the circle and the effect of changing the angle of the attached mass segment on the fundamental frequencies is investigated. The property of the Heaviside function has been used to investigate the effect of the attached mass.

The Heaviside function affects the integral intervals when solving the governing equations of the shell with the attached mass. These integrals in the longitudinal and circumferential directions represent the dimensions of the attached mass or the overall dimensions of the structure. Stiffness and mass matrices are obtained by multiplying these integrals in the matrix of material properties and surface unit density, respectively. By keeping the position of the attached mass constant in the longitudinal direction, the only variable in this section is the increase in the subtended angle of the coupled mass. Increasing the semi-vertex angle causes the corresponding integrals to be increased and this effect on the shell stiffness is greater than the effect of its mass, which has led to an increase in the fundamental frequencies of the composite cone, according to Table 8.

Figure 6 investigates the effect of the placement of a ring at different longitudinal distances on the conical shell on the fundamental frequencies for longitudinal wave $m = 1$. Increasing the distance from the small end side of the cone to 0.4 of the total length of the shell increases the natural frequency and beyond this value, it decreases the natural frequency. Because by increasing the radius of the cone at different longitudinal distances, the size of the ring

becomes larger and as a result, the mass increases. In fact, up to x/L=0.4, the effect of the stiffness matrix is more than the mass matrix, and therefore the frequency is increased and beyond x/L=0.4, the effect of the mass matrix is greater than the stiffness, which causes the natural frequencies to be decreased. In this section, in all cases, the length, angle, density, and height of the attached mass are constant and the effective factor in changing the integrals is the radius of the cone. In some integrals, increasing the radius, increases and in others decreases the value of the integral, but in integrals related to the mass matrix, it only increases the mass.

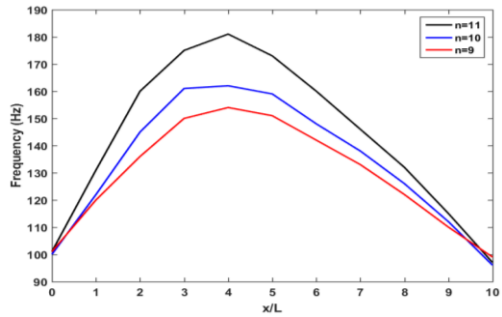

Fig 6. Effect of the place of the attached mass on the shells natural frequencies; The shell is made of material no. 1 and geometry no. 1, $\varphi=15°$; The attached mass is made of material no. 2, m=1, $L_a=0.05m$, $h_a=0.01m$, $\theta_a=2\pi$

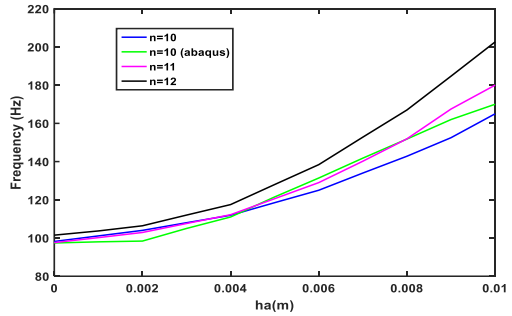

Fig 7. Effect of thickness of the attached mass on the shells natural frequencies; The shell is made of material no. 1 and geometry no. 1, $\varphi=15°$; The attached mass is made of material no. 2, $L_a=0.05m$, $\theta_a=2\pi$

Figure 7 indicates the effect of coupled mass thickness on the base frequencies. By increasing the thickness, the frequency of the structure is increased. In this case, the thickness affects the stiffness and mass matrices, so that in the stiffness matrix, it has the greatest effect on the flexural stiffness section, causing the component (D_{11}) to increase 34 times. However, increasing the thickness from 0.002m to 0.01m causes the mass to be increased by five times. Accordingly, the frequency is increased by 1.6, 1.75, and 1.9 times for n=10, n=11, and n=12, respectively.

Shells used in different industries may have equipment attached inside the shell. If the area of the installation of the equipment is stiffened enough and the mass of the equipment is considered to be distributed over that area, its mass effect can be calculated by increasing the area density and the result of free vibrations can be examined. Table 9 investigates the effect of increasing the density of a ring in the middle of the cone on the fundamental frequencies of the shell. The fundamental frequency occurred when no mass was added $\rho=0\left(kg/m^3\right)$. Increasing the density directly affects the shell mass matrix and reduces the fundamental frequencies. In the first stage ($\rho=2710kg/m^3$), mass was added to the shell along with stiffness and hence caused the fundamental frequencies of the shell to be increased. In this study, the mass of the shell is 22.5 kg. By changing the density of the attached mass, the mass of the ring increases from 1.92 to 19.47 kg. In the next step, by increasing the density ($\rho=13550kg/m^3$ and $\rho=27100kg/m^3$) the fundamental frequency is decreased and for the density $\rho=13550kg/m^3$, the fundamental frequency occurred at *n*=10.

Table 10 indicates the effect of increasing the modulus of elasticity of a ring in the middle of a conical shell. Increasing Young's modulus of the attached mass increases the values of the stiffness in the tangential direction according to Eq. (17) and thus increases the overall stiffness of the system. Accordingly, the stiffness matrix K_{ij} in Eq. (14) is affected considering the attached mass. Hence, the increased overall stiffness also increases the fundamental frequencies of the system. In this case, the components of the material matrix are increased up to four times.

Table 8. Effect of attached mass subtended angle on the shell's natural frequencies. The shell is made of material no. 1 and geometry no. 1, $\varphi=45^{\circ}$; The attached mass is made of material no. 2, $L_a=0.05\ m$, $h_a=0.01\ m, m=1$

	θ_a (deg)	**n=10**	**n=11**	**n=12**	M_a/M_s
	0	97.68	97.02	100.52	0
	30	108.14	110.93	122.75	0.03
	60	124.62	123.99	138.07	0.07
Present Analytical	90	129.50	137.21	150.05	0.11
	180	146.39	157.86	174.91	0.21
	270	157.35	171.05	190.57	0.32
	360	165.08	180.24	201.42	0.43
Present ABAQUS	360	169.77	177.48	179.61	0.43

Table 9. Effect of the density of the attached mass on the shell's natural frequencies. The shell is made of material no. 1 and geometry no. 1, $\varphi = 15°$; The attached mass is made of material no. 2, $L_a = 0.05m$, $h_a = 0.002m$, $\theta_a = 2\pi$

	$\rho(kg/m^3)$	**0**	**2710**	**13550**	**27100**
n=10	Present Analytical	98.11	104.01	78.58	66.86
	Present ABAQUS	97.68	98.30	81.44	64.77
	Discrepancy(%)	0.46	5.48	3.5	3.22
n=11	Present Analytical	97.49	102.88	80.90	66.13
	Present ABAQUS	97.02	100.81	80.55	66.72
	Discrepancy(%)	0.48	2.01	0.43	0.88
n=12	Present Analytical	101.07	106.30	86.57	68.33
	Present ABAQUS	100.52	107.39	83.23	71.39
	Discrepancy(%)	0.54	1.01	4.01	4.28

Table 10. Effect of Young's modulus of the attached mass on the shell's natural frequencies. The shell is made of material no. 1 and geometry no. 1, $\varphi = 15°$; The attached mass is made of material no. 2, $L_a = 0.05m$, $h_a = 0.002m$, $\theta_a = 2\pi$

	$E\,(GPa)$	**0**	**70**	**140**	**210**	**280**
Present Analytical	n=10	98.11	104.01	115.35	125.49	134.72
	n=11	97.49	102.88	113.57	123.03	131.56
	n=12	101.07	106.3	116.98	126.28	134.90
Present ABAQUS	n=12	100.52	107.39	114.25	118.6	121.74
Discrepancy(%)		0.54	1.1	2.33	6.08	9.75

Figure 8 shows the twelfth mode (n=12) obtained from ABAQUS software for $E = 70GPa$ and longitudinal wave number m=1.

Figure 9 presents the effect of increasing the width of the ring located in the middle of the conical shell. By changing the longitudinal place of the attached mass, the amount of integrals in the stiffness and mass matrix becomes larger. On the other hand, the thickness and properties of the material are constant in this case. As a result, increasing the length causes the values of the stiffness and mass matrices to be increased. The effect of this parameter on the stiffness matrix is greater and therefore increases the fundamental frequencies of the shell. In Figure 10, the effect of adding a narrow attached mass in the longitudinal direction (stringer) at different subtended angles on the natural frequencies of the shell is indicated. The geometrical and mechanical properties of the shell are geometrical No.1 in Table 2 and material No. 1 in Table 1, respectively. The mechanical properties of the attached mass are material No. 2 in Table 1. It can be seen, at small circumferential wave number (n), the effect of the angle change is insignificant on the natural frequency, but at large circumferential wave number (n) and near the fundamental frequency, the effect of the cone angle change on the natural frequency is significant.

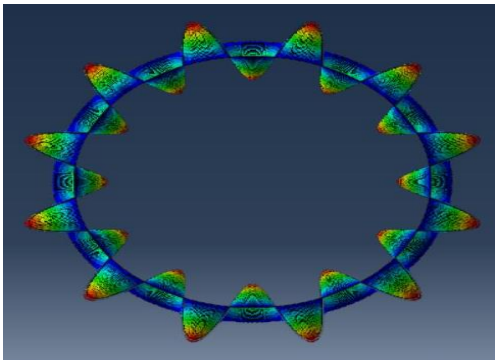

Fig. 8. The twelfth mode (n=12) obtained from ABAQUS software for longitudinal wave number m=1 and $E = 70GPa$

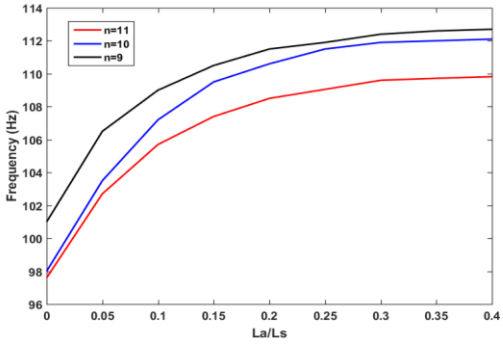

Fig 9. Effect of the length of the attached mass to the cone length on the shells natural frequencies; The shell is made of material no. 1 and geometry no. 1, $\varphi = 15°$; The attached mass is made of material no. 2, $h_a = 0.002m, \theta_a = 2\pi$

7-3- Investigation of the Effect of Length and Thickness of Shell on the Natural Frequencies

The influence of geometrical parameters (h/R_1) and (L/R_1) on the natural frequency is investigated. That R_1 is the small radius and t thickness of the conical shell. Fig. 11 Indicated the effect of (h/R_1) on the natural frequency. It can be seen, at small circumferential wave numbers $(n \le 4)$, the effect of increasing (h/R_1) is insignificant on the natural frequency, but at large circumferential wave number $(n > 4)$, the effect of increasing (h/R_1), is significant on the natural frequency.

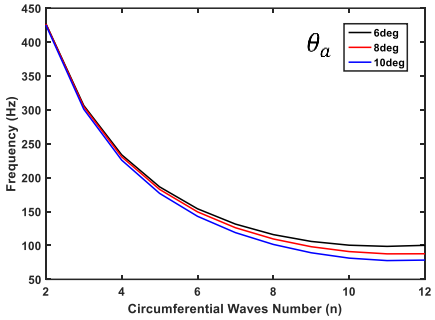

Fig 10. Effect of attached mass subtended angle on the natural frequencies of the cone stiffened with a stringer in the longitudinal direction (stringer). $L_a = L_s$, $h_a = 0.002\,m$

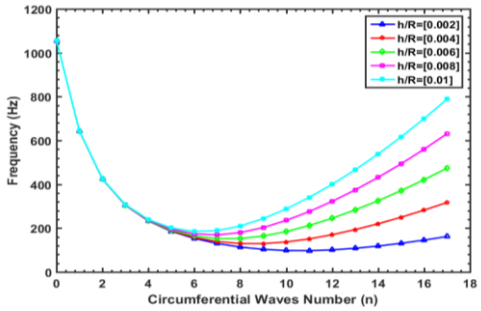

Fig 11. Effect of the ratio of thickness to small radius (h/R_1) on the natural frequency; The shell is made of material no. 1 and $R_1 = 1m$, $m = 1$, $L = 1m$, $\varphi = 15^0$ and orientation $[90/0/90/0/90/0]$

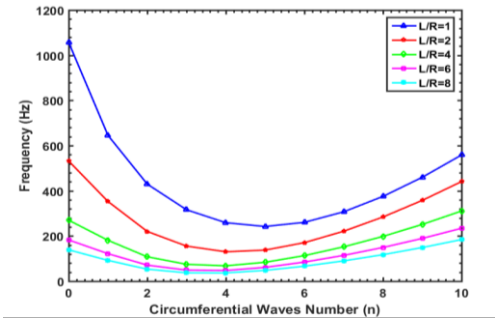

Fig 12. Effect of the ratio of length to small radius (L/R_1) on the natural frequency; The shell is made of material no. 1 and $R_1 = 1m$, $m = 1$, $t = 0.02\,m$, $\varphi = 15^0$ and orientation $[90/0/90/0/90/0]$

Also increasing the ratio of length to small radius (L/R_1) on the natural frequency of the composite conical shell is shown in Figure 12. It can be seen, increasing the ratio of length to small radius at different circumferential wave numbers reduces the natural frequency of the system. Given that the length parameter at the integrals of the free vibration section of the cone is often Located at the denominator of the fraction, this decrease in frequency in exchange for an increase in length is justified. Also in the low circumferential wave number, with the increasing length of the shell (increasing the ratio of length to radius) the rate of decrease in natural frequency is greater than in the case that the number of the circumferential wave is larger.

8. Conclusion

In this paper, for the first time, the free vibrations of the conical shell with a locally attached mass are investigated. The equilibrium equations of the composite conical shell are obtained based on the classical theory of shells and using the energy method and Hamilton's principle. The boundary conditions of the shell are considered to be simply supported. The displacement components are written in the form of double Fourier series according to the boundary conditions. The relations of displacement-strain and displacement-curvature are considered based on Love's first approximation. Using Galerkin's method, the governing equations of the free vibrations of the conical shell are solved and the natural frequencies, the mode shapes, and the effect of different parameters on them are investigated. Also, the effect of attached mass using the cone differential operator and the effect of the Heaviside function on the equilibrium equations have been considered and its effect on the free vibrations of the conical shell has been investigated. Validation of the obtained results has been done with the aid of references and ABAQUS finite element software. In the following, the most important results and outcomes of the present study are stated as the following:

1- Increasing the subtended angle of the attached mass causes the frequencies to be increased.
2- The effect of placement of a ring in the longitudinal direction up to about x/L=0.4 of the shell length increases the fundamental frequencies and beyond x/L=0.4 causes the fundamental frequencies to be decreased.
3- Increasing the thickness of the attached mass in the fundamental modes has increased the frequencies.
4- Increasing the width of the attached mass from 5 to 40 percent of the shell length has

increased the integrals in the stiffness and mass matrices, which has led to an increase in the fundamental frequencies of the cone.

5- Placing the attached mass in the longitudinal direction of the shell and at different subtended angles has little effect on the first circumferential wave number and has a decreasing effect on the greater circumferential wave numbers as well as the fundamental frequencies.

6- Increasing the ratio of length to radius of shell in all circumferential wave numbers reduces the natural frequency of the shell

Appendix A:

$$\bar{Q}_{11} = Q_{11}c^4 + 2\left(Q_{12} + 2Q_{33}\right)s^2c^2 + Q_{22}s^4$$
$$\bar{Q}_{12} = \left(Q_{11} + Q_{22} - 4Q_{33}\right)s^2c^2 + Q_{12}\left(s^4 + c^4\right)$$
$$\bar{Q}_{22} = Q_{11}s^4 + 2\left(Q_{12} + 2Q_{33}\right)s^2c^2 + Q_{22}c^4$$
$$\bar{Q}_{13} = \left(Q_{11} - Q_{12} - 2Q_{33}\right)sc^3 + \left(Q_{12} - Q_{22} + 2Q_{33}\right)s^3c$$
$$\bar{Q}_{23} = \left(Q_{11} - Q_{12} - 2Q_{33}\right)s^3c + \left(Q_{12} - Q_{22} + 2Q_{33}\right)sc^3$$
$$\bar{Q}_{33} = \left(Q_{11} + Q_{22} - 2Q_{12} - 2Q_{33}\right)s^2c^2 + Q_{33}\left(s^4 + c^4\right)$$
$$c = Cos\theta \quad , \quad s = Sin\theta$$
$$Q_{11}^k = \frac{E_1}{1-\upsilon_{12}\upsilon_{21}} \quad , \quad Q_{12}^k = \frac{\upsilon_{12}E_1}{1-\upsilon_{12}\upsilon_{21}}$$
$$Q_{22}^k = \frac{E_2}{1-\upsilon_{12}\upsilon_{21}} \quad , \quad Q_{33}^k = G_{12}$$

(That the subscript “k” is the layer number).

Appendix B:

$$L_{11} = A_{11}\frac{\partial^2}{\partial x^2} + \frac{2A_{16}}{R}\frac{\partial^2}{\partial x\partial\theta} + \frac{A_{11}s}{R}\frac{\partial}{\partial x} - \frac{A_{22}s^2}{R^2} + \frac{A_{66}}{R^2}\frac{\partial^2}{\partial\theta^2}$$

$$L_{12} = \frac{B_{16}\cdot c}{R}\frac{\partial^2}{\partial x^2} - \frac{A_{22}\cdot s}{R^2}\frac{\partial}{\partial\theta} - \frac{A_{26}\cdot s}{R}\frac{\partial}{\partial x} + \frac{A_{26}\cdot s^2}{R^2} - \frac{A_{66}\cdot s}{R^2}\frac{\partial}{\partial\theta} + \frac{B_{26}\cdot c}{R^3}\frac{\partial^2}{\partial\theta^2} + \frac{B_{66}\cdot c}{R^2}\frac{\partial^2}{\partial x\,\partial\theta} + \frac{A_{12}}{R}\frac{\partial^2}{\partial x\,\partial\theta} + \frac{B_{12}\cdot c}{R^2}\frac{\partial^2}{\partial x\,\partial\theta} - \frac{B_{12}\cdot c\cdot s}{R^3}\frac{\partial}{\partial\theta} + \frac{A_{66}}{R}\frac{\partial^2}{\partial x\,\partial\theta} + \frac{A_{26}}{R^2}\frac{\partial^2}{\partial\theta^2} - \frac{2B_{16}\cdot c\cdot s}{R^2}\frac{\partial}{\partial x} + \frac{2B_{16}\cdot s^2\cdot c}{R^3} - \frac{B_{22}s\cdot c}{R^3}\frac{\partial}{\partial\theta} - \frac{B_{26}\cdot s\cdot c}{R^2}\frac{\partial}{\partial x} + \frac{2B_{26}\cdot s^2\cdot c}{R^3} - \frac{2B_{66}\cdot s\cdot c}{R^3}\frac{\partial}{\partial\theta} + A_{16}\frac{\partial^2}{\partial x^2}$$

$$L_{13} = -\frac{3B_{16}}{R}\frac{\partial^3}{\partial x^2\partial\theta} - \frac{B_{26}}{R^3}\frac{\partial^3}{\partial\theta^3} - \frac{2B_{66}}{R^2}\frac{\partial^3}{\partial x\,\partial\theta^2} - \frac{B_{12}}{R^2}\frac{\partial^3}{\partial x\,\partial\theta^2} - \frac{A_{22}\cdot s\cdot c}{R^2} + \frac{A_{12}\cdot c}{R}\frac{\partial}{\partial x} + \frac{B_{12}\cdot s}{R^3}\frac{\partial^2}{\partial\theta^2} + \frac{2B_{16}\cdot s}{R^2}\frac{\partial^2}{\partial x\,\partial\theta} - \frac{2B_{16}\cdot s^2}{R^3}\frac{\partial}{\partial\theta} - \frac{B_{11}\cdot s}{R}\frac{\partial^2}{\partial x^2} + \frac{B_{22}\cdot s}{R^3}\frac{\partial^2}{\partial\theta^2} + \frac{B_{22}\cdot s^2}{R^2}\frac{\partial}{\partial x} + \frac{B_{26}\cdot s}{R^2}\frac{\partial^2}{\partial x\,\partial\theta} - \frac{2B_{26}\cdot s^2}{R^3}\frac{\partial}{\partial\theta} + \frac{A_{26}\cdot c}{R^2}\frac{\partial}{\partial\theta} + \frac{2B_{66}\cdot s}{R^3}\frac{\partial^2}{\partial\theta^2} - B_{11}\frac{\partial^3}{\partial x^3}$$

$$L_{21} = A_{16}\frac{\partial^2}{\partial x^2} + \frac{A_{26}\cdot s^2}{R^2} + \frac{A_{26}\cdot s}{R}\frac{\partial}{\partial x} + \frac{A_{66}\cdot s}{R^2}\frac{\partial}{\partial\theta} + \frac{A_{66}}{R}\frac{\partial^2}{\partial x\,\partial\theta} + \frac{A_{12}}{R}\frac{\partial^2}{\partial x\,\partial\theta} + \frac{A_{22}\cdot s}{R^2}\frac{\partial}{\partial\theta} + \frac{A_{26}}{R^2}\frac{\partial^2}{\partial\theta^2} + \frac{2A_{16}\cdot s}{R}\frac{\partial}{\partial x} + \frac{B_{12}\cdot c}{R^2}\frac{\partial^2}{\partial x\,\partial\theta} + \frac{B_{22}\cdot s\cdot c}{R^3}\frac{\partial}{\partial\theta} + \frac{B_{26}\cdot c}{R^3}\frac{\partial^2}{\partial\theta^2} + \frac{2B_{16}\cdot c\cdot s}{R^2}\frac{\partial}{\partial x} + \frac{B_{26}\cdot c\cdot s^2}{R^3} + \frac{B_{66}\cdot c\cdot s}{R^3}\frac{\partial}{\partial\theta} + \frac{B_{16}\cdot c}{R}\frac{\partial^2}{\partial x^2} + \frac{B_{26}\cdot c\cdot s}{R^2}\frac{\partial}{\partial x} + \frac{B_{66}\cdot c}{R^2}\frac{\partial^2}{\partial x\,\partial\theta}$$

$$L_{22} = \frac{2A_{26}}{R}\frac{\partial^2}{\partial x\,\partial\theta} - \frac{2B_{26}\cdot c\cdot s}{R^3}\frac{\partial}{\partial\theta} + \frac{4B_{26}\cdot c}{R^2}\frac{\partial^2}{\partial x\,\partial\theta} + \frac{2B_{22}\cdot c}{R^3}\frac{\partial^2}{\partial\theta^2} + \frac{D_{22}\cdot c^2}{R^4}\frac{\partial^2}{\partial\theta^2} + \frac{2D_{26}\cdot c^2}{R^3}\frac{\partial^2}{\partial x\,\partial\theta} + \frac{D_{66}\cdot c^2}{R^2}\frac{\partial^2}{\partial x^2} + \frac{A_{66}\cdot s}{R}\frac{\partial}{\partial x} - \frac{A_{66}\cdot s^2}{R^2} + \frac{2B_{66}\cdot c}{R}\frac{\partial^2}{\partial x^2} + A_{66}\frac{\partial^2}{\partial x^2} + \frac{A_{22}}{R^2}\frac{\partial^2}{\partial\theta^2} - \frac{B_{66}\cdot s^2\cdot c}{R^3} - \frac{2D_{26}\cdot c^2\cdot s}{R^4}\frac{\partial}{\partial\theta} - \frac{D_{66}\cdot c^2\cdot s}{R^3}\frac{\partial}{\partial x}$$

$$L_{23} = -\frac{B_{26}\cdot s^2}{R^2}\frac{\partial}{\partial x} + \frac{A_{22}\cdot c}{R^2}\frac{\partial}{\partial\theta} + \frac{B_{22}\cdot c^2}{R^3}\frac{\partial}{\partial\theta} + \frac{B_{26}\cdot c^2}{R^2}\frac{\partial}{\partial x} + \frac{2B_{26}\cdot s}{R^3}\frac{\partial^2}{\partial\theta^2} - \frac{B_{26}\cdot s}{R}\frac{\partial^2}{\partial x^2} - \frac{B_{22}\cdot s}{R^2}\frac{\partial^2}{\partial x\,\partial\theta} - \frac{2B_{16}\cdot s}{R}\frac{\partial^2}{\partial x^2} - \frac{D_{12}\cdot c}{R^2}\frac{\partial^3}{\partial x^2\partial\theta} - \frac{D_{22}\cdot c}{R^4}\frac{\partial^3}{\partial\theta^3} - \frac{3D_{26}\cdot c}{R^3}\frac{\partial^3}{\partial x\,\partial\theta^2} - \frac{D_{16}\cdot c}{R}\frac{\partial^3}{\partial x^3} - \frac{2D_{66}\cdot c}{R^2}\frac{\partial^3}{\partial x^2\partial\theta} - \frac{3B_{26}}{R^2}\frac{\partial^3}{\partial x\,\partial\theta^2} - \frac{2B_{66}}{R}\frac{\partial^3}{\partial x^2\partial\theta} - \frac{B_{12}}{R}\frac{\partial^3}{\partial x^2\partial\theta} - \frac{B_{22}}{R^3}\frac{\partial^3}{\partial\theta^3} - B_{16}\frac{\partial^3}{\partial x^3} + \frac{A_{26}\cdot c}{R}\frac{\partial}{\partial x} + \frac{A_{26}\cdot c\cdot s}{R^2} - \frac{D_{22}\cdot c\cdot s}{R^3}\frac{\partial^2}{\partial x\,\partial\theta} + \frac{2D_{26}\cdot c\cdot s}{R^4}\frac{\partial^2}{\partial\theta^2} - \frac{2D_{16}\cdot c\cdot s}{R^2}\frac{\partial^2}{\partial x^2} - \frac{D_{26}\cdot c\cdot s}{R^2}\frac{\partial^2}{\partial x^2} + \frac{B_{26}\cdot c^2\cdot s}{R^3} - \frac{D_{26}\cdot c\cdot s^2}{R^3}\frac{\partial}{\partial x}$$

$$L_{31} = B_{11}\frac{\partial^3}{\partial x^3} - \frac{A_{12}\cdot c}{R}\frac{\partial}{\partial x} - \frac{A_{26}\cdot c}{R^2}\frac{\partial}{\partial\theta} + \frac{B_{22}\cdot s^3}{R^3} + \frac{B_{26}\cdot s^2}{R^3}\frac{\partial}{\partial\theta} + \frac{2B_{11}\cdot s}{R}\frac{\partial^2}{\partial x^2} - \frac{B_{22}\cdot s^2}{R^2}\frac{\partial}{\partial x} + \frac{B_{26}\cdot s}{R^2}\frac{\partial^2}{\partial x\,\partial\theta} + \frac{B_{22}\cdot s}{R^3}\frac{\partial^2}{\partial\theta^2} + \frac{3B_{16}}{R}\frac{\partial^3}{\partial x^2\partial\theta} + \frac{2B_{66}}{R^2}\frac{\partial^3}{\partial x\,\partial\theta^2} + \frac{B_{12}}{R^2}\frac{\partial^3}{\partial x\,\partial\theta^2} + \frac{B_{26}}{R^3}\frac{\partial^3}{\partial\theta^3} - \frac{A_{22}\cdot c\cdot s}{R^2} + \frac{2B_{16}\cdot s}{R^2}\frac{\partial^2}{\partial x\,\partial\theta}$$

$$L32 = \frac{2D_{12}\cdot c\cdot s^2}{R^4}\frac{\partial}{\partial\theta} + \frac{B_{12}}{R}\frac{\partial^3}{\partial x^2\partial\theta} - \frac{2D_{12}\cdot c\cdot s}{R^3}\frac{\partial^2}{\partial x\,\partial\theta}$$
$$+B_{16}\frac{\partial^3}{\partial x^3} + \frac{D_{12}\cdot c}{R^2}\frac{\partial^3}{\partial x^2\partial\theta} + \frac{B_{22}}{R^3}\frac{\partial^3}{\partial\theta^3} + \frac{3B_{26}}{R^2}\frac{\partial^3}{\partial x\,\partial\theta^2} +$$
$$\frac{2B_{66}}{R}\frac{\partial^3}{\partial x^2\partial\theta} - \frac{B_{22}\cdot s}{R^2}\frac{\partial^2}{\partial x\,\partial\theta} - \frac{B_{26}\cdot s}{R}\frac{\partial^2}{\partial x^2} -$$
$$\frac{B_{26}\cdot s}{R^3}\frac{\partial^2}{\partial\theta^2} + \frac{3D_{26}\cdot c}{R^3}\frac{\partial^3}{\partial x\,\partial\theta^2} + \frac{2D_{66}\cdot c}{R^2}\frac{\partial^3}{\partial x^2\partial\theta} +$$
$$\frac{D_{22}\cdot c}{R^4}\frac{\partial^3}{\partial\theta^3} + \frac{B_{16}\cdot s}{R}\frac{\partial^2}{\partial x^2} + \frac{D_{16}\cdot c}{R}\frac{\partial^3}{\partial x^3} - \frac{A_{22}\cdot c}{R^2}\frac{\partial}{\partial\theta}$$
$$-\frac{A_{26}\cdot c}{R}\frac{\partial}{\partial x} - \frac{B_{22}\cdot c^2}{R^3}\frac{\partial}{\partial\theta} - \frac{B_{26}\cdot c^2}{R^2}\frac{\partial}{\partial x} + \frac{B_{22}\cdot s^2}{R^3}\frac{\partial}{\partial\theta}$$
$$+\frac{B_{26}\cdot s^2}{R^2}\frac{\partial}{\partial x} - \frac{B_{26}\cdot s^3}{R^3} - \frac{D_{22}\cdot s\cdot c}{R^3}\frac{\partial^2}{\partial x\,\partial\theta} -$$
$$\frac{D_{26}\cdot s\cdot c}{R^2}\frac{\partial^2}{\partial x^2} - \frac{4D_{26}\cdot c\cdot s}{R^4}\frac{\partial^2}{\partial\theta^2} - \frac{4D_{66}\cdot c\cdot s}{R^3}\frac{\partial^2}{\partial x\,\partial\theta}$$
$$-\frac{2D_{16}\cdot c\cdot s}{R^2}\frac{\partial^2}{\partial x^2} + \frac{2D_{22}\cdot s^2\cdot c}{R^4}\frac{\partial}{\partial\theta} + \frac{3D_{26}\cdot s^2\cdot c}{R^3}\frac{\partial}{\partial x} -$$
$$\frac{4D_{26}\cdot s^3\cdot c}{R^4} + \frac{4D_{66}\cdot s^2\cdot c}{R^4}\frac{\partial}{\partial\theta} + \frac{A_{26}\cdot c\cdot s}{R^2} + \frac{2B_{26}\cdot c^2\cdot s}{R^3}$$
$$+\frac{4D_{16}\cdot c\cdot s^2}{R^3}\frac{\partial}{\partial x} - \frac{4D_{16}\cdot s^3\cdot c}{R^4}$$

$$L_{33} = -\frac{2B_{26}\cdot c\cdot s}{R^3}\frac{\partial}{\partial\theta} + \frac{B_{22}\cdot s^2\cdot c}{R^3} - \frac{4D_{66}}{R^2}\frac{\partial^4}{\partial x^2\partial\theta^2}$$
$$-\frac{D_{22}}{R^4}\frac{\partial^4}{\partial\theta^4} - \frac{2D_{12}}{R^2}\frac{\partial^4}{\partial x^2\partial\theta^2} - \frac{4D_{16}}{R}\frac{\partial^4}{\partial x^3\partial\theta} - \frac{4D_{26}}{R^3}\frac{\partial^4}{\partial x\,\partial\theta^3}$$
$$-\frac{A_{22}\cdot c^2}{R^2} + \frac{4D_{16}\cdot s^3}{R^4}\frac{\partial}{\partial\theta} - \frac{D_{22}\cdot s^3}{R^3}\frac{\partial}{\partial x} + \frac{4D_{26}s^3}{R^4}\frac{\partial}{\partial\theta} -$$
$$D_{11}\frac{\partial^4}{\partial x^4} + \frac{2B_{22}\cdot c}{R^3}\frac{\partial^2}{\partial\theta^2} + \frac{4B_{23}\cdot c}{R^2}\frac{\partial^2}{\partial x\,\partial\theta} + \frac{2D_{12}\cdot s}{R^3}\frac{\partial^3}{\partial x\,\partial\theta^2}$$
$$-\frac{2D_{12}\cdot s^2}{R^4}\frac{\partial^2}{\partial\theta^2} - \frac{4D_{16}\cdot s^2}{R^3}\frac{\partial^2}{\partial x\,\partial\theta} - \frac{2D_{11}\cdot s}{R}\frac{\partial^3}{\partial x^3} -$$
$$\frac{2D_{22}\cdot s^2}{R^4}\frac{\partial^2}{\partial\theta^2} + \frac{D_{22}\cdot s^2}{R^2}\frac{\partial^2}{\partial x^2} - \frac{4D_{26}\cdot s^2}{R^3}\frac{\partial^2}{\partial x\,\partial\theta} +$$
$$\frac{2B_{12}\cdot c}{R}\frac{\partial^2}{\partial x^2} + \frac{4D_{26}\cdot s}{R^4}\frac{\partial^3}{\partial\theta^3} + \frac{4D_{66}\cdot s}{R^3}\frac{\partial^3}{\partial x\,\partial\theta^2} -$$
$$\frac{4D_{66}\cdot s^2}{R^4}\frac{\partial^2}{\partial\theta^2}$$

(That $c = \cos\varphi$ and $s = \sin\varphi$)

References

[1] Tong, L., 1993. Free vibration of composite laminated conical shells, *Int. J. Mech. Sci.*, 35, pp. 47–61.

[2] Shu, C., 1996. Free Vibration analysis of Composite Laminated Conical Shelle by Generalized differential Quadrature. *J. Sound Vib.*, 194, pp. 587–604.

[3] Li, F.-M., Kishimoto, K. and W.-H. Huang, W.-H., 2009. The calculations of natural frequencies and forced vibration responses of conical shell using the Rayleigh–Ritz method, *Mech. Res. Commun.*, 36, pp. 595–602.

[4] Jin, G., Ma, X., Shi, S., Ye, T. and Liu, Z., 2014. A modified Fourier series solution for vibration analysis of truncated conical shells with general boundary conditions, *Appl. Acoust.*, 85, pp. 82–96.

[5] Nasiri Rad, A., Ansari, R. and Rouhi, H., 2013. Free and Forced Vibration Analysis of Composite Conical Shell Under Different Boundary Condition Via Galerkin Method, *Journal of Solid Mechannics in Engineering*, 6, pp. 23-35.

[6] L. Nallim, L., Grossi, R. O. and Laura, P. A. A., 1998. Transverse Vibration of Cicular Plates of Rectangular Orthotropy Carring a Central Concentrated Mass, *J. Sound Vib.*, 216, pp. 337–341.

[7] Bambill, D. V., La Malfa,S., Rossit, C. A. and Laura, P. A. A., 2004. Analytical and experimental investigation on transverse vibrations of solid, circular and annular plates carrying a concentrated mass at an arbitrary position with marine applications, *Ocean Eng.*, 31, pp. 127–138.

[8] Amabili, M., Pellegrini, M., Righi, F. and Vinci, F., 2006. Effect of concentrated masses with rotary inertia on vibrations of rectangular plates, *J. Sound Vib.*, 295, pp. 1–12.

[9] Ciancio, P. M., Rossit, C. A. and Laura, P. A. A., 2007. Approximate study of the free vibrations of a cantilever anisotropic plate carrying a concentrated mass, *J. Sound Vib.*, 302, pp. 621–628.

[10] Khalili, S. M. R., Tafazoli, S. and Malekzadeh Fard, K., 2011. Free vibrations of laminated composite shells with uniformly distributed attached mass using higher order shell theory including stiffness effect, *J. Sound Vib.*, 330, pp. 6355–6371.

[11] Aksencer, T. and Aydogdu, M., 2018. Vibration of a rotating composite beam with an attached point mass, *Compos. Struct.*, 190, pp. 1–9.

[12] Qu, Y., Wu, S., Chen, Y. and HUa, H., 2013. Vibration analysis of ring-stiffend conical-cylindrical-spherical shells based on a modified variational approach, *International journal of mechanical Sciences*, 69, pp. 72-84.

[13] Nekouei, M., Raghebi, M. and Mohammadi, M., 2019. Free vibration analysis of laminated composite conical shells reinforced with shape memory alloy fibers, *Acta Mechanica*, 230, pp. 4235-4255.

[14] Song, Z., Cao, Q. and Dai, Q., 2019. Free vibration of truncated conical shells with elastic boundary constraints and added mass, *International Journal of Mechanical Sciences,* 155, pp. 286-294.

[15] S. M. R. Khalili, S. M. R., Azarafza, R. and Davar, A., 2009. Transient dynamic response of initially stressed composite circular

cylindrical shells under radial impulse load, *Compos. Struct.*, 89, pp. 275–284.

[16] Jin, G., Ye, T. and Su, Z., 2015. *Structural vibration: a uniform accurate solution of laminated beams, plates and shells with general boundary conditions*, 1st ed. Springer-Verlag Berlin Heidelberg.

[17] Azarafza, R., Khalili, S. M. R., Jafari, A. A. and Davar, A., 2009. Analysis and optimization of laminated composite circular cylindrical shell subjected to compressive axial and transverse transient dynamic loads, *Thin-Walled Struct.*, 47, pp. 970–983.

[18] Jafari, A. A. and Bageri, M., 2006. Free vibration of non- uniformly ring stiffened cylindrical shells using analytical, experimental and numerical methods, *Thin-Walled Struct.,* 44, pp. 82–90.